

Intra-Pulse Radar-Embedded Communications

Shannon D. Blunt *Senior Member, IEEE*, Padmaja Yatham *Member, IEEE*,
and James Stiles *Senior Member, IEEE*,

This work was supported in part by the Office of Naval Research (ONR 31) and the Air Force Office of Scientific Research.

S.D. Blunt and J. Stiles are with the Radar Systems & Remote Sensing Lab (RSL) and the Dept. of Electrical Engineering and Computer Science (EECS) at the University of Kansas, Lawrence, KS.

P. Yatham is with the Sprint Nextel Corporation, Overland Park, KS.

Abstract

The embedding of a covert communication signal amongst the ambient scattering from an incident radar pulse has previously been achieved by modulating a Doppler-like phase shift sequence over numerous pulses (*i.e.* on an *inter*-pulse basis). In contrast, this paper considers radar-embedded communications on an *intra*-pulse basis whereby an incident radar waveform is converted into one of K communication waveforms, each of which acts as a communication symbol representing some pre-determined information (*e.g.* a bit sequence). To preserve a low intercept probability this manner of radar-embedded communications necessitates prudent selection of the set of communication waveforms as well as interference cancellation on receive. A general mathematical model and subsequent optimization problem is established for the design of the communication waveforms, from which three design strategies are developed. Also, receiver design issues are discussed and an interference-canceling maximum likelihood receiver is presented. Performance results are presented in terms of the communication symbol error rate as well as a correlation-based metric from which intercept probability can be inferred. It is demonstrated that, given persistent radar illumination with a pulse repetition frequency (PRF) of 1-2 kHz, *intra*-pulse radar-embedded communications can theoretically achieve data-rates commensurate with speech coding (for the interval of the radar dwell time) with the potential for even higher data-rates if additional diversity is appropriately incorporated.

Keywords

Radar-embedded communications, RFID, retro-reflector, radar responsive tag, Intra-pulse modulation, waveform design, interference cancellation

I. INTRODUCTION

The ability to communicate covertly is essential for defense-related applications where an intercepted message could be exploited by an adversary to reveal sensitive information and/or the existence and location of key resources. Traditional means of covert communication rely on active signaling whereby the signal is designed to rapidly "hop" around the spectrum or to appear noise-like [1]. However, an alternative approach is to exploit an existing signal emitted from another transmitter by re-radiating the incident signal after it has been "re-modulated" into a different form by a radio frequency (RF) tag/transponder such that the new signal now conveys some desired information. As long as it is properly designed, this new signal could likewise simply be transmitted after being triggered by the incident illumination (for proper timing to maintain covert nature). Detection of the communication signal within the ambient electromagnetic environment can be quite difficult for an adversary because the embedded signal,

if selected appropriately, can possess lower power than the clutter produced by natural scattering and still be recovered by the intended receiver.

Pulsed radar is an attractive choice for an existing transmitter to exploit as it can operate over a considerable range with high illumination power, tends to employ moderately high bandwidths (from 1-2 MHz for surveillance to 100's of MHz for imaging), and has a repeating structure from pulse-to-pulse thus enabling relative ease of synchronization. Because the embedded communication signal must, at the receiver, be in some way separable from the ambient radar scattering, the degrees-of-freedom within which a communication signal may feasibly exist are thus dictated by the characteristics of the particular radar as well as by the phenomenological properties of the illuminated scatterers. Conceptually, these degrees-of-freedom include frequency (spectral "location" and bandwidth), polarization, spatial selectivity, Doppler or azimuth (for pulse-Doppler or synthetic aperture radar (SAR), respectively), and range (delay shift and fast-time "waveform-domain" modulation). Hence, in theory there exists a high-dimensional space, only partially occupied by the ambient radar scattering, where the embedded communication signal may reside. However, to utilize the "masking" benefit of the radar scattering and thereby preserve a low intercept probability, this high-dimensional space must be properly constrained such that the embedded communication signal is only separable from the ambient scattering via coherent receive processing with the known set of communication signals. Also note that when relying on pulsed radar to establish a masking signal based on scattering, practicality limits operation to the backscatter regime where clutter exists over a considerable delay spread. The delay spread in the forward scatter regime is dictated by any multipath components, which will generally provide a very short delay spread relative to the backscatter regime.

The general notion of "re-modulating" an incident signal as a means of conveying information was first proposed by Stockman in 1948 [2]. Depending on the particular application, variations of this technology are now referred to as radar tags/transponders, retrodirective arrays, retro-reflectors, or most commonly as radio frequency identification (RFID). Tags can range in sophistication [3] from simple passive reflectors that contain no power source other than the incident illumination, to semi-passive reflectors that power internal circuitry with a battery, to active transponders that supply additional gain to the reflected signal. It should also be noted that the embedded communication method presented here does not necessarily require reflection of the incident radar waveform as the communication signaling may alternatively involve completely

active transmission (*i.e.* without reflection) after being triggered by an incident pulse (this could be accomplished via, for example, something similar to a Digital RF Memory (DRFM) device [4]). However, for the sake of brevity we shall herein simply use the nomenclature of a *tag* to refer to the communication device.

In regard to the degrees-of-freedom mentioned above, polarization-based RF tags have been utilized to calibrate polarimetric radar for remote sensing applications [5]-[8]. RF tags have also been used to impart a phase-shift sequence over numerous (typically 100's) of pulses to insert target identification/location information into SAR images via coherent integration of the embedded signal in the azimuth domain [9]-[13]. Most notably, tags of the inter-pulse type have been developed to prevent battlefield "friendly fire" incidents. Because these *inter*-pulse approaches typically encode over 100's of pulses, often denoted as a coherent processing interval (CPI), the embedded signal can have a very low probability of intercept (LPI). However, this desirable attribute is obtained at the cost of very low data-rates on the order of bits-per-CPI which effectively translates to just a few bits-per-second (bps). At the other extreme, if the LPI benefit of the masking interference is disregarded (*e.g.* the tag frequency shifts the incident signal completely out-of-band) and/or if the radar illumination is rather simple, such as for a continuous-wave (CW) Doppler radar, data-rates on the order of Mbps can be obtained [14], [15].

In contrast to previous work, this paper considers the utility of radar-embedded communications on an *intra*-pulse basis (*i.e.* at the waveform level) whereby each incident radar pulse (modulated with some phase- or frequency-coded waveform) is re-modulated into one of K different communication waveforms¹. The set of K possible communication waveforms represent the K communication symbols that may be encoded for each incident pulse, thus realizing a data-rate on the order of bits-per-pulse. Most pulsed radar systems operate with a pulse repetition frequency (PRF) on the order of kHz, thus the resulting overall data-rate can be measured in kbps which is analogous to speech coding based on the MELP codec [18]-[20] (for the time interval of the radar dwell time). Also, note that unlike the azimuth/Doppler-based *inter*-pulse schemes [9]-[13], re-modulating on an *intra*-pulse basis effectively eliminates degradation due to receiver Doppler mismatch induced by tag motion as the time baseline for a communication

¹Originally presented at the 2007 Waveform Diversity & Design Conf. [16] with additional mathematical derivation presented at the 2007 IEEE Intl. Conf. on Electromagnetics in Advanced Applications. [17]

symbol is now considerably shorter.

For the intra-pulse framework, low intercept probability is facilitated through the proper design of the set of communication waveforms. While these waveforms should have minimal correlation (or better yet orthogonality) with one another to maintain a low communication error rate, they should also possess some nominal correlation with the surrounding radar reflections such that they cannot be discerned from the ambient scattering without prior knowledge of their specific form. Furthermore, the degree of correlation between a communication waveform and the ambient scattering should be approximately the same over the set of communication waveforms so as not to bias the symbol estimation process on receive. Given prior knowledge of the set of K possible communication waveforms as well as the illuminating radar waveform, the receive estimation of the particular embedded communication waveform is accomplished via interference cancellation. Thus unlike traditional LPI communications which rely upon the concept of low energy density in the spectrum, intra-pulse radar-embedded communications maintains a low intercept probability by forcing an intercept receiver to extricate the communication signal from a masking interference signal, which is extremely difficult without prior knowledge of the nature of the embedded signal.

From a practical viewpoint, a valid question is whether the radiated energy from a tag/transponder is sufficient for signal detection. The answer of course is highly scenario dependent, determined from parameters such as target range, transmit power, antenna gain and aperture, processing gain, data rate, and error requirements. System performance likewise depends on the design parameters of the tag itself. Because a tag collects and then re-radiates electromagnetic energy, an equivalent radar cross-section (RCS), denoted as σ , can be determined for a given tag. With respect to a system power budget calculation, a convenient way of evaluating tag performance is with RCS. For example, a tag with a relatively small antenna effective aperture of $A_e = \lambda^2$ exhibits a radar cross-section of $\sigma = 4\pi\lambda^2 G_{RF}$ where G_{RF} denotes the RF gain (or loss) through the tag. An active tag can thus be used to enhance RCS. For example, at 3.0 GHz this antenna effective aperture would be $A_e = 100 \text{ cm}^2$. If the tag is active with an RF gain of 17 dB, it would have an RCS of more than 6 square meters – a value considered to be more than sufficiently large for most radar applications.

The purpose of this paper is to develop the theoretical framework for intra-pulse radar-embedded communications and to discuss the general issues that will impact feasible imple-

mentation, some of which remain open research topics. The remainder of the paper is organized as follows. Section II develops a general mathematical formulation for intra-pulse re-modulation and defines a constrained optimization problem for communication waveform design. Section III presents three strategies for communication waveform design and discusses their relative merits and limitations. In Section IV the design of an appropriate interference cancellation receiver is discussed and one such receiver is presented based on the code-division multiple-access (CDMA) decorrelating detector formulation [21],[22]. Also, a metric is developed from which the probability of intercept can be inferred. Section V discusses some practical implementation issues for intra-pulse radar embedded communications. Finally, Section VI presents simulation results for the proposed communication waveform design strategies and interference-canceling receiver in terms of communication error rate and the proposed metric for intercept probability.

II. INTRA-PULSE RE-MODULATION

A typical pulsed-radar waveform can be characterized by its center frequency, polarization, and by a phase/frequency modulation over the extent of the pulse, which translates into some bandwidth about the given center frequency. The received reflections from this illumination are thus expected to be delayed versions of the same phase/frequency modulation and thus occupy the same bandwidth, though the received polarization can be arbitrary as it also depends on the illuminated scatterers.

Using the illuminating radar waveform as a reference, a tag can modulate the reflection of the incident radar waveform into one of K possible communication waveforms. The communication waveform is thus embedded into the ambient scattering that acts as masking interference to maintain a low intercept probability. Mathematically, this manner of radar-embedded communications can be represented in the following manner. Let $s(t)$ be the transmitted radar waveform which illuminates a collection of discrete, linear *time-invariant* scatterers. The response at the radar receiver (or at some other intended receiver) can thus be described by:

$$y_s(t) = \int_V \int \psi_{\text{rx}}(t, t'; \bar{r}) \int \gamma_s(\bar{r}) \delta(t' - t'') dt' \int \psi_{\text{tx}}(t'', t'''; \bar{r}) s(t''') dt'' dt''' d\bar{r} = s(t) * x(t) \quad (1)$$

where the functions ψ_{tx} and ψ_{rx} describe the propagation from the radar antenna to a particular scatterer at position \bar{r} within volume V and back, respectively, $\delta(\cdot)$ is the dirac delta, and t' , t'' , and t''' are the relative time of reflection by a scatterer, incidence at a scatterer, and initial transmission by the radar, respectively. The complex value γ_s indicates the scattering coefficient

of the discrete scatterer. Additionally, given that the ambient scattering can be assumed to be a linear time-invariant process (the contribution from moving targets is assumed negligible), the received signal due to clutter can be expressed as a convolution of the radar waveform $s(t)$ and the aggregation of scattering in terms of fast-time which is denoted as $x(t)$.

In contrast to the phenomenology of ambient scattering, the tag is essentially a discrete, linear *time-varying* scatterer. If located at position \bar{r} , the k^{th} possible received response $c_k(t)$ from this object is, to within a scale factor,

$$c_k(t) = \int \psi_{\text{rx}}(t, t'; \bar{r}) \int \phi_k(t', t'') dt' \int \psi_{\text{tx}}(t'', t'''; \bar{r}) s(t''') dt'' dt''' = s(t) \times \phi_k(t) \quad (2)$$

where the kernel $\phi_k(t, t')$ describes the k^{th} re-modulation operation upon the incident waveform $s(t)$ thus yielding the k^{th} communication waveform $c_k(t)$ for $k = 1, 2, \dots, K$. This re-modulation operation, which is applicable for the passive implementation, is simply obtained as $\phi_k(t) = c_k(t) \div s(t)$ according to the designed communication waveforms $c_k(t)$. The received response $y_r(t)$ resulting from a single tag located within a collection of scattered objects is therefore

$$y_r(t) = \alpha_k c_k(t) + y_s(t) + n(t) \quad (3)$$

with $n(t)$ being additive noise and α_k denoting the combined effect of the transmit strength of the tag, path loss, and constructive/destructive interference due to multipath. Note that $\alpha_\ell = 0$ for $\ell \neq k$ (*i.e.* the other $K - 1$ that are not currently transmitted). Thus, presuming accurate estimation of α_k for $k = 1, \dots, K$, the intended receiver can discern which of the K waveforms was transmitted by evaluating $\max\{|\alpha_1|, \dots, |\alpha_K|\}$. To illustrate the general operation of the proposed form of embedded communication, Fig. 1 depicts the convolution and modulation operations of the ambient clutter and tag, respectively, along with fading effects and additive noise. Note that, because it is not particularly important for the development here, the attenuation of clutter due to path loss is simply subsumed into the backscatter. It should also be noted that the received signal model of (3) is also applicable when the tag/transponder actively transmits a communication waveform instead of passively re-modulating the incident radar waveform.

From the standpoint of optimal estimation of the embedded communication waveform, the k^{th} re-modulation operation would ideally “rotate” the illuminating function $s(t)$ into a subspace orthogonal to the responses from the surrounding scatterers, *i.e.*

$$\int c_k(t) y_s^*(t) dt = 0, \quad (4)$$

while likewise producing a communication waveform that is mutually orthogonal to the other $K - 1$ communication waveforms such that

$$\int c_j(t) c_k^*(t) dt = 0 \quad \text{for } j \neq k \quad (5)$$

where $(\cdot)^*$ denotes complex conjugation. However, to preserve the LPI attribute of the set of communication waveforms, they must remain partially correlated with the radar scatter so that an intercept receiver cannot simply project away the radar illumination from the received signal $y_r(t)$ and thereby uncover the embedded communication signal (this issue is discussed in Section IV). Thus, from the perspective of optimizing the estimation of the correct embedded communication waveform given that some degree of correlation with the radar scatter is necessary, an optimization problem for communication waveform design can be expressed as:

$$\begin{aligned} & \min_{c_1 \cdots c_K} \left[\sum_{j=1}^K \sum_{k=1}^K \left| \int c_j(t) c_k^*(t) dt \right| - \sum_{j=1}^K \int c_j(t) c_j^*(t) dt \right] \\ & \text{such that } \int c_k(t) y_s^*(t) dt = \beta \int y_s(t) y_s^*(t) dt \quad \text{for } k = 1, 2, \dots, K. \end{aligned} \quad (6)$$

In other words, minimize the cross-correlation between the communication waveforms to thereby minimize symbol errors on receive while maintaining the normalized correlation between each communication waveform and the radar scattering to be equal to the constant β such that the LPI characteristic is maintained. In practice, the exact ambient scattering $y_s(t)$ may not be accessible and hence a direct solution of (7) is not feasible. Thus it will be shown in the next section how the illuminating radar waveform $s(t)$ may be utilized to approximately achieve the constraints “on average” and also thereby enable a more feasible heuristic implementation.

Under the assumption that the communication waveforms meet the above requirements (at least approximately), exact knowledge of the set of K communication waveforms $c_0(t), \dots, c_{K-1}(t)$ is required to determine which was conveyed by the tag. In the presence of the radar scatter interference and noise, this determination necessitates coherent processing of the received signal. Thus, given a set of K filters $w_0(t), \dots, w_{K-1}(t)$, the estimation of the particular embedded communication waveform can be performed as

$$\hat{k} = \arg \max_k \left| \int w_k(t) y_r^*(t) dt \right| \quad (7)$$

where \hat{k} is the index of the waveform determined to be present. If standard matched filtering is used then $w_k(t) = c_k(t)$. However, because matched filtering does not account for the presence of interference [21], it is expected that poor communication error performance will result unless the embedded signal has a power level that is commensurate with the ambient scattering, in which case the embedded signal is not LPI. In Section IV, it is discussed how the communication error performance for a low-power embedded signal (and thus LPI) can be improved significantly by using receive filters that provide some degree of interference cancelation.

III. COMMUNICATION WAVEFORM DESIGN

Intra-pulse radar-embedded communications operates by re-modulating an incident radar waveform into one of K different communication waveforms. For a receiver to recover the embedded signal, the set of communication waveforms must be both sufficiently separable from one another in order to minimize symbol estimation errors and sufficiently separable from the ambient radar scattering in order to minimize the effects of interference. Of course, if the communication waveforms are too different from the ambient scattering (*e.g.* frequency shifted out of band) then the natural masking supplied by the radar scatter cannot be exploited. As such, a logical choice is to generate communication waveforms that reside in (or very near to) the passband of the incident radar illumination yet are “temporally coded” in such a way as to possess a manageable level of correlation with the radar scattering. In this work we shall consider temporal coding in terms of (fast-time) phase and amplitude modulation of the incident radar waveform. Note that it is assumed here that both the tag and the intended receiver (which could be the illuminating radar) obtain identical copies of the incident radar waveform. In practice, the incident radar illumination may contain some forward scatter (multipath) effects. The communication waveform design approaches described here are applicable when the multipath components can be neglected relative to the direct path radar waveform.

In general, radar waveforms fully occupy their passband thus leaving no spectral region within the passband in which to embed a communication waveform. Stated another way, this spectral occupancy implies that insufficient design degrees-of-freedom exist with which to generate a communication waveform that solely occupies the radar passband. However, it is well known that radar emissions are not strictly confined to their passband and exhibit a “spreading” effect into the surrounding spectrum [25] as depicted in Fig. 2. This effect can be exploited to provide a covert region very near to the radar passband in which the embedded communication signal

can reside. Furthermore, by allowing the bandwidth of the communication waveforms to be marginally larger than that of the radar illumination, additional degrees-of-freedom become available with which to design suitable communication waveforms.

While one could inject any given signal to act as a communication waveform, a more deliberate design strategy may be employed to ensure that the embedded communication signal is sufficiently separable from the ambient scattering while also maintaining a nominal level of similarity with the ambient scattering to ensure a low intercept probability. We shall consider three particular approaches to communication waveform design, all of which are based on an eigen-decomposition of the collection of delay shifts of the incident radar waveform thereby modeling the aggregate set of ambient radar reflections. Note that this approach is applicable to both "continuous" and "discrete" radar waveforms as long as the entire waveform bandwidth is taken into account (*i.e.* the "extraneous" bandwidth due to transitions for discrete waveforms).

Consider a radar waveform $s(t)$ having a bandwidth B that is illuminating a given area. A tag within the illuminated area can obtain a discrete representation of the radar waveform by sampling the incident illumination at the Nyquist rate of B complex samples/second. The length of the resulting Nyquist-sampled waveform is denoted as N . Of course, at the Nyquist sampling rate the radar waveform completely occupies the discrete spectrum. To accommodate the design of appropriate communication waveforms, the incident illumination is alternatively sampled at a rate of MB complex samples/second where M is an over-sampling factor and dictates how much additional spectrum is to be utilized to embed a communication waveform. Thus the length of the over-sampled discrete representation of $s(t)$ is NM .

Let us denote the vector $\mathbf{s} = [s_0 \ s_1 \ \cdots \ s_{NM-1}]^T$ as the factor-of- M over-sampled discrete representation of the radar waveform where $(\cdot)^T$ is the transpose operation. Bearing in mind the communication waveform optimization problem defined in (7), we shall consider a design framework based on manipulation of the vector space established by the temporal autocorrelation of a model for the ambient scattering $y_s(t)$. The continuous radar scattering model of (1) can be discretely represented as the convolution of the discretized radar waveform \mathbf{s} and a discretized version of the aggregate ambient scattering. This convolution operation can alternatively be

expressed as a matrix multiplication of the form

$$\mathbf{S}\mathbf{x} = \begin{bmatrix} s_{NM-1} & s_{NM-2} & \cdots & s_0 & 0 & \cdots & 0 \\ 0 & s_{NM-1} & & s_1 & s_0 & & 0 \\ \vdots & & \ddots & \vdots & \vdots & \ddots & \\ 0 & 0 & & s_{NM-1} & s_{NM-2} & \cdots & s_0 \end{bmatrix} \mathbf{x} \quad (8)$$

where \mathbf{x} is a length $2NM-1$ vector comprised of range samples of the aggregate ambient radar scattering and the $NM \times (2NM-1)$ matrix \mathbf{S} contains shifted versions of the illuminating radar waveform. Knowledge of the particular values in \mathbf{x} is not required in order to design appropriate communication waveforms, though the average power of the scattering in a particular direction may be utilized to control the power level of the embedded signal.

Using the discrete ambient scattering framework of (8), a convenient basis within which to generate sets of communication waveforms can be obtained by computing the eigen-decomposition of the correlation of \mathbf{S} as

$$\mathbf{S}\mathbf{S}^H = \mathbf{V}\mathbf{\Lambda}\mathbf{V}^H \quad (9)$$

where $\mathbf{V} = [\mathbf{v}_0 \ \mathbf{v}_1 \ \cdots \ \mathbf{v}_{NM-1}]$ contains the NM eigenvectors, $\mathbf{\Lambda}$ is a diagonal matrix comprised of the associated eigenvalues (assumed to be in order of increasing magnitude), and $(\cdot)^H$ is the complex-conjugate transpose, or Hermitian, operator. As an example, consider the over-sampling of a linear frequency modulated (LFM) radar waveform. It is known that a Nyquist-sampled version of an LFM is embodied by the Lewis-Kretschmer P3 and P4 codes based on single-sideband and double-sideband modulation, respectively [26]. Thus we may obtain an over-sampled version of an LFM by over-sampling the mathematical function for either the P3 or P4 code. For an over-sampling factor of $M = 2$ and the P3 code with a Nyquist-sampled length of $N = 100$, Fig. 3 depicts the resulting eigenvalues in dB scale. Note that the dominant portion of the eigen-spectrum is approximately rank N and is relatively flat while the remaining non-dominant portion of the eigen-spectrum exhibits a much greater dynamic range. It is within this non-dominant space that we shall design and embed communication waveforms via the associated eigenvectors. As such, the waveform design process can be tailored to produce communication waveforms that possess low correlation (or are even orthogonal) while also possessing near-equal correlation with the ambient scattering on average.

For now, it is assumed that the tag and the intended receiver each obtain an identical over-sampled discrete representation of the illuminating radar waveform and thus an identical set of

eigenvectors \mathbf{V} . The justification for this assumption is based on the fact that radar illumination is generally very high power and has undergone only one-way path loss. We shall consider the case of offset between the tag sampling and the receiver sampling in Section V. Based on the set of eigenvalues, three communication waveform design approaches are proposed. Also, based on the notion of the dominant and non-dominant spaces of the radar scattering, a simple metric to ascertain the probability of intercept for intra-pulse radar-embedded communications is discussed.

A. Eigenvectors-as-Waveforms (EAW)

The straightforward approach to communication waveform design/selection is to directly utilize a subset of the non-dominant eigenvectors as communication waveforms. To minimize the effects of interference biasing the receiver communication symbol estimates in (7) due to inequitable correlation with the ambient radar scattering, the eigenvectors to be selected as waveforms should be associated with eigenvalues that are of near-equal magnitude. This near-equality may typically be achieved by selecting the eigenvectors associated with the K smallest eigenvalues as

$$\mathbf{c}_k = \mathbf{v}_k \quad \text{for } k = 1, 2, \dots, K. \quad (10)$$

These eigenvectors possess the least correlation with the ambient scattering (they are in fact virtually orthogonal to the clutter) and, as such, tend to yield the lowest communication error rate since the interference has the least impact on receiver performance of the three communication waveform design methods considered here.

In terms of intercept probability, the EAW approach can be problematic because the correlation of the communication waveforms with the ambient scattering is low so that interference biasing does not occur. Thus, the EAW waveforms may be easy to discern. In contrast, the two other approaches for communication waveform design utilize a larger portion of the eigen-spectrum to “spread” the waveforms throughout the available design space thereby significantly reducing the intercept probability.

B. Weighted-Combining (WC)

As a trade-off to generate communication waveforms that are more covert at the cost of a slightly higher receive error rate, we consider the weighted combining of multiple non-dominant eigenvectors. Denoting a set of L non-dominant eigenvectors as $\tilde{\mathbf{V}}_{\text{ND}} = [\mathbf{v}_0 \quad \mathbf{v}_1 \quad \dots \quad \mathbf{v}_{L-1}]$, a

set of K communication waveforms can be formed by combining the L non-dominant eigenvectors as

$$\mathbf{c}_k = \tilde{\mathbf{V}}_{\text{ND}} \mathbf{b}_k \quad \text{for } k = 1, 2, \dots, K \quad (11)$$

where each \mathbf{b}_k is a different $L \times 1$ weight vector known only to the tag and to the intended receiver.

Because the set of L non-dominant eigenvectors can correspond to a larger spread of eigenvalue magnitudes, the resulting communication waveforms will generally be more correlated with the radar scattering. Thus, relative to the previous EAW approach, the weighted-combining approach yields a lower intercept probability at the cost of a slightly higher communication error rate. By selecting the weight vectors \mathbf{b}_k to contain relatively constant modulus terms, the set of K communication waveforms \mathbf{c}_k will be equally correlated with the ambient radar scattering on average. Furthermore, if the set of K weight vectors are orthogonal, then it can be readily shown that the resulting set of communication waveforms will be orthogonal as long as $K \leq L$. Therefore, the receiver error rate can be managed at the tag by controlling the power of the embedded signal relative to the radar interference. Also, the increased correlation with the radar scattering, which provides the lower intercept probability, necessitating interference cancellation to extract the embedded signal.

C. Dominant-Projection (DP)

Finally, instead of concentrating upon the non-dominant space in order to generate the communication waveforms, we shall consider the projection away from the dominant space. This approach becomes particularly useful in situations where relative sampling offsets of the incident radar waveform may result in a slightly different representation of \mathbf{s} for the tag and the intended receiver thus producing some variations in the set of eigenvectors (discussed in detail in Section V). The dominant-projection approach considers the dominant space as a whole and thus is less susceptible than the other two approaches to differences in (and ordering of) individual eigenvectors.

The dominant projection approach to communication waveform design utilizes a set of K pseudo-random $NM \times 1$ vectors denoted as \mathbf{d}_k , for $k = 1, 2, \dots, K$, that are known to both the tag and the intended receiver. For the first L eigenvectors of \mathbf{V} corresponding to the non-dominant space and the remaining $NM - L$ eigenvectors corresponding to the dominant space

(note that the size of L is somewhat arbitrary), the first communication waveform is found as

$$\mathbf{c}_1 = \left(\mathbf{I} - \tilde{\mathbf{V}}_{D,0} \tilde{\mathbf{V}}_{D,0}^H \right) \mathbf{d}_1 \quad (12)$$

where $\tilde{\mathbf{V}}_{D,0} = \begin{bmatrix} \mathbf{v}_L & \mathbf{v}_{L+1} & \cdots & \mathbf{v}_{NM-1} \end{bmatrix}$ is the $NM - L$ eigenvectors comprising the dominant space of \mathbf{V} . To obtain the second communication waveform, the $NM \times 1$ communication waveform \mathbf{c}_1 is appended to the $NM \times (2NM - 1)$ matrix \mathbf{S} such that the $NM \times 2NM$ matrix

$$\mathbf{S}_{P,1} = \begin{bmatrix} \mathbf{S} & \mathbf{c}_1 \end{bmatrix} \quad (13)$$

is formed and subsequently used to obtain a new eigen-decomposition as

$$\mathbf{S}_{P,1} \mathbf{S}_{P,1}^H = \mathbf{V}_{P,1} \mathbf{\Lambda}_{P,1} \mathbf{V}_{P,1}^H. \quad (14)$$

The second communication waveform is then found as

$$\mathbf{c}_2 = \left(\mathbf{I} - \tilde{\mathbf{V}}_{D,1} \tilde{\mathbf{V}}_{D,1}^H \right) \mathbf{d}_2 \quad (15)$$

where $\tilde{\mathbf{V}}_{D,1} = \begin{bmatrix} \mathbf{v}_{L-1} & \mathbf{v}_L & \cdots & \mathbf{v}_{NM-1} \end{bmatrix}$ is the $NM - L + 1$ eigenvectors comprising the dominant space of $\mathbf{V}_{P,1}$. Note that to accommodate the inclusion of the communication waveform \mathbf{c}_1 , the rank of the dominant space has been incremented by 1. In general, the k^{th} communication waveform is obtained by determining the eigen-decomposition of the correlation of the $NM \times (2NM + k - 1)$ matrix

$$\mathbf{S}_{P,k} = \begin{bmatrix} \mathbf{S} & \mathbf{c}_1 & \cdots & \mathbf{c}_k \end{bmatrix} \quad (16)$$

and then projecting out the dominant $NM - L + k - 1$ eigenvectors from the vector \mathbf{d}_k . The result of this sequential design process is that the set of K communication waveforms are orthogonal and, as long as K is not overly large, have approximately the same correlation with the ambient scattering.

IV. RECEIVER OPERATION

Embedding a communication waveform into the spectral region immediately surrounding the radar passband provides a natural means with which to maintain a low intercept probability due to the masking ‘‘interference’’ provided by the radar. However, this interference introduces some obstacles at the intended receiver that must be addressed in order to ensure satisfactory communication performance as measured by the symbol-error-rate (SER) or bit-error-rate (BER).

Over the time interval within which the embedded communication signal arrives at the intended receiver, the total received discretized signal of length NM (assuming synchronization) has the form

$$\mathbf{y}_r = \alpha_k \mathbf{c}_k + \mathbf{S}\mathbf{x} + \mathbf{n} \quad (17)$$

where \mathbf{n} is a vector of NM additive noise samples. To ensure a low intercept probability, the received power of the embedded signal \mathbf{c}_k must remain sufficiently below that of the masking radar scatter resulting from the $\mathbf{S}\mathbf{x}$ term. As such, because it cannot account for the presence of this significant interference term, the standard coherent filter matched to \mathbf{c}_k may not provide adequately low communication error performance. However, the received signal model of (17) has distinct parallels to CDMA multi-user detection [21], thus numerous estimators already exist that may be exploited to extract the embedded communication signal. Also, we shall use (17) to develop a straight-forward intercept metric.

A. Receiver Design

Due to its relative simplicity and because it does not require knowledge of relative power levels, we shall use the maximum likelihood receiver (also known as the decorrelating receiver [21],[22] in the CDMA nomenclature). It is assumed that the intended receiver possesses exact knowledge of the set of communication waveforms as well as knowledge of the illuminating radar waveform. The $NM \times (2NM + K - 1)$ matrix \mathbf{C} can thus be formed by appending the K communication waveforms as columns to the radar-waveform delay-shift matrix \mathbf{S} as

$$\mathbf{C} = \left[\mathbf{S} \quad \mathbf{c}_1 \quad \cdots \quad \mathbf{c}_K \right] \quad (18)$$

which models all the possible signal components (radar backscatter and communications) that may be present in the received signal \mathbf{y}_r . Then, under the assumption that the noise term in (17) is white Gaussian, the pdf of the total received signal \mathbf{y}_r parameterized on $\mathbf{b} = [\mathbf{x}^T \alpha_1 \cdots \alpha_K]^T$ can be expressed as

$$p(\mathbf{y}_r; \mathbf{b}) = \frac{1}{(\pi \sigma_v^2)^{NM}} \exp \left\{ -\frac{1}{\sigma_v^2} (\mathbf{y}_r - \mathbf{C}\mathbf{b})^H (\mathbf{y}_r - \mathbf{C}\mathbf{b}) \right\}. \quad (19)$$

The maximum likelihood estimate of \mathbf{b} can therefore be obtained by minimizing the term $(\mathbf{y}_r - \mathbf{C}\mathbf{b})^H (\mathbf{y}_r - \mathbf{C}\mathbf{b})$ which yields

$$\hat{\mathbf{b}} = (\mathbf{C}\mathbf{C})^{-1} \mathbf{C}^H \mathbf{y}_r. \quad (20)$$

Since we are only concerned with obtaining estimates for the set of K possible communication waveforms, the k^{th} decorrelating filter is thus

$$\mathbf{w}_k = (\mathbf{C}\mathbf{C}^H)^{-1} \mathbf{c}_k \quad (21)$$

for $k = 1, 2, \dots, K$. Extraction of the embedded communication signal is then achieved by selecting the communication symbol that satisfies

$$\hat{k} = \arg \left\{ \max_k \left\{ \left| \mathbf{w}_k^H \mathbf{y}_r \right| \right\} \right\}. \quad (22)$$

Because it effects a cancellation of the portion of the dominant subspace that is occupied by the clutter, the processing gain of the decorrelating filter is approximately the dimensionality of the non-dominant subspace.

The maximum likelihood (decorrelating) receiver of (21) is known to be the minimum variance unbiased (MVU) estimator of \mathbf{b} for the linear model in (17) [23]. The decision rule in (22) is the minimum distance receiver [24] for multiple hypothesis detection. However, it should be noted that this decision rule does not account for the null hypothesis (*i.e.* none of the communication waveforms are present/detectable). Given the requirement to maintain a low probability of intercept the power of the embedded signal is necessarily low relative to the ambient clutter. Therefore, it would be prudent in practice to ascertain the likelihood of a communication waveform being present in addition to determining which of the K possible waveforms is most likely.

B. Intercept Receiver

Because intra-pulse radar-embedded communications operates by inserting a communication waveform in and around the spectrum already occupied by the ambient radar scattering, the classical notions of intercept probability based on the measurement of spectral energy content are no longer applicable. From a conceptual standpoint, a general metric for the intercept probability of these interference-masked signals must in some way account for the ambient radar scattering and also should utilize no knowledge of the communication waveforms. The authors are not aware of any such metric currently in existence.

A simple metric that is related to intercept probability can be obtained if one allows the intercept receiver to possess some prior knowledge. If it is assumed that the intercept receiver has knowledge of the over-sampling factor M employed by the tag and the intended receiver, then

an eigen-decomposition can be performed as in (9). Using the set of eigenvectors, a normalized correlation metric based on a projection of the received signal onto the non-dominant space can be obtained in the following manner.

The $NM \times j$ matrix $\tilde{\mathbf{V}}_D$ is formed from the j eigenvectors corresponding to the j largest eigenvalues. As such, $\tilde{\mathbf{V}}_{D,j}$ represents a dominant subspace of rank j . A projection matrix is formed for each $j \in [1, \dots, NM]$ as

$$\mathbf{P}_j = \mathbf{I} - \tilde{\mathbf{V}}_{D,j} \tilde{\mathbf{V}}_{D,j}^H. \quad (23)$$

The j^{th} projection matrix \mathbf{P}_j is applied to the received signal \mathbf{r} to obtain the j^{th} projection residue as

$$\tilde{\mathbf{z}}_j = \mathbf{P}_j \mathbf{y}_r \quad (24)$$

from which the normalized correlation with the k^{th} communication waveform, which we shall denote as $\eta_{k,j}$, is determined as

$$\eta_{k,j} = \frac{|\mathbf{c}_k^H \tilde{\mathbf{z}}_j|}{\sqrt{(\mathbf{c}_k^H \mathbf{c}_k) (\tilde{\mathbf{z}}_j^H \tilde{\mathbf{z}}_j)}}. \quad (25)$$

While this metric does not directly determine the probability of intercept, it allows one to infer the degree to which an intercept receiver could accurately extract a communication waveform that has been embedded among the ambient radar scattering. Higher values of η indicate a greater similarity to the embedded signal. As will be demonstrated in Section VI, this metric justifies the use of the weighted-combining (WC) and dominant-projection (DP) waveform design approaches because, even though they yield somewhat higher error rates than the eigenvalues-as-waveforms (EAW) approach, these techniques effectively preclude the intercept receiver from obtaining the set of communication waveforms.

V. IMPLEMENTATION ISSUES

The primary issues regarding practical implementation of intra-pulse modulation for radar-embedded communications are 1) establishment of an appropriate reflected power level, 2) synchronization with the incident illumination for both the tag and the intended receiver, and 3) synchronization of the intended receiver with the received embedded signal. The reflected power from the tag should be sufficiently large relative to the noise and ambient radar scattering so as to provide a low communication error rate at the intended receiver. However, the embedded

signal power must also remain sufficiently below that of the ambient scattering power to maintain a low intercept probability. It is for this reason that interference cancellation (such as the decorrelating receiver discussed in Section IV.A) becomes necessary so as to contend with low signal-to-clutter ratio (SCR). Of course, due to the natural time-varying nature of the environment there will be times in which the signal undergoes fading so as to induce an SCR that is insufficient to maintain the communication link. Error correction coding, interleaving, etc may be employed to remediate these effects to some degree.

Setting the appropriate power level for the embedded signal is further complicated by the fact that ambient scattering is generally directionally dependent. The method developed herein is particularly designed for the backscatter regime (operation in the radar forward scatter regime may further complicate the demands on low intercept probability). A simple solution to aid in proper selection of the signal power level is to self-generate a masking clutter signal which can be accomplished via a Digital RF Memory (DRFM) device [4]. Generally considered an Electronic Countermeasure, the DRFM may operate in concert with the tag to ensure a proper SCR level and, as will be discussed below, may additionally aid in synchronization with the desired receiver.

In regard to synchronization with the incident radar illumination, the tag and intended receiver would ideally trigger on the leading edge of the incident pulse to begin sampling the radar waveform. Otherwise, a relative sampling offset occurs and the tag and receiver obtain versions of the sampled radar waveform \mathbf{s} that are slightly different. This difference in the respective representations of the radar waveform would result in differences in the respective eigen-decompositions of (9). As such, the set of communication waveforms possessed by the intended receiver would not exactly match those embedded by the tag which may thereby produce some performance degradation at the receiver. In Section VI, the effects of relative sampling offsets are examined for the three communication waveform design techniques. It is found that the dominant-projection approach, because it addresses an eigenvector subspace instead of the individual eigenvectors, is more robust to sampling offset than the other two waveform design techniques.

Finally, it has been assumed throughout the paper that the intended receiver is synchronized with the incident signal containing the given embedded communication waveform. However, in practice it is possible that the receiver will possess only approximate knowledge of the time interval in which the embedded signal resides. Note that this approximate timing knowledge may be obtained if the tag uses, for example, the location/identification capability provided by *inter-*

pulse modulation techniques [9]-[13]. In fact, if combined with a pulse-to-pulse phase modulation sequence, the masking clutter provided by a DRFM that was discussed above may be exploited to establish synchronization of the tag with the intended receiver. Given sufficient memory, once the intended receiver determines the the presence of a tag, it may scan back through collected data to extract the higher data-rate embedded signal for each pulse. Of course, some fast-time (i.e. range domain) ambiguity may still exist. Thus, given some approximate interval within which the embedded signal may reside, the received signal model of (17) may be expanded as

$$\mathbf{y}_r(\ell) = \alpha_k \mathbf{c}_k(\ell) + \mathbf{S}\mathbf{x}(\ell) + \mathbf{n}(\ell) \quad (26)$$

where ℓ denotes a relative delay-shift index and $\mathbf{c}_k(\ell)$ is a NM -length delay-shifted version of \mathbf{c}_k with the remainder zero-filled. Based on this model the receiver must therefore also expand the maximization procedure of (22) to account for nearby delay shifts as

$$\hat{k} = \arg \left\{ \max_{k,\ell} \left\{ \left| \mathbf{w}_k^H \mathbf{y}_r(\ell) \right| \right\} \right\}. \quad (27)$$

Therefore, in this context the design of appropriate communication waveforms must account for what is essentially a range ambiguity issue that is a consequence of (27). This issue remains as future work to be addressed.

VI. SIMULATION RESULTS

To simulate the theoretical performance for intra-pulse radar-embedded communications we consider an incident radar waveform that is linearly frequency modulated (LFM) which, when sampled at Nyquist, yields a length $N = 100$ nominally-sampled discrete representation (modeled using the mathematical function for the P3 code [26]). Note that similar results as those shown here have been observed for other common radar waveforms as well. The incident waveform is over-sampled by a factor of $M = 2$ at the tag. The number of communication waveforms (symbols) is set to $K = 4$ so that 2 bits of information are conveyed upon the re-modulated reflection of each incident pulse. It has been observed that, to within the dimensionality limits of the non-dominant eigenspace, a doubling of the number of communication waveforms (and thus an increase of 1 bit of information) translates into roughly a 3 dB degradation in symbol-error-rate (SER) performance. From (17), the ambient radar scatter \mathbf{x} and noise \mathbf{n} are modeled as white Gaussian. The average power of the embedded communication signal, the ambient radar scatter (the interference), and the noise are each scaled to achieve the desired levels of

signal-to-clutter ratio (SCR) and signal-to-noise ratio (SNR).

An example of a communication waveform is depicted in Fig. 4 when using the Dominant Projection approach (the waveform is normalized to possess unit norm). To the degree that the incident radar waveform is band-limited, so too is the communication waveform that is based on the eigen-decomposition of the factor-of- M over-sampled version of the radar waveform. It is found that the communication waveforms fill the remainder of the digital spectrum that is not occupied by the over-sampled radar waveform. In other words, the eigen-based design approaches effectively perform "water-filling" in the digital spectrum. Thus, relative to the analog pass-band of the radar waveform, the communication waveforms occupy the nearby spectral "shoulders".

The eigenvectors-as-waveforms (EAW) approach uses the 1st four eigenvectors as these correspond to the eigenvalues with the most commensurate magnitudes within the non-dominant space. The other two approaches set $L = 100$ as the size of the non-dominant space for the purpose of communication waveform design. Note that as a result, the communication waveforms for weighted-combining (WC) and dominant-projection (DP) possess a non-trivial correlation with the radar illumination. As such, interference cancellation is necessary to sufficiently extricate the embedded signal. The sets of weight vectors \mathbf{b}_k and pseudo-random vectors \mathbf{d}_k for the WC and DP approaches, respectively, are both drawn from complex Gaussian distributions.

For each of the waveform design techniques, the SNR is varied for particular values of SIR to ascertain the relative communication symbol-error-rate (SER). Each SER value estimated by simulating 100,000 independent "symbols". Also, using communication waveform $k = 1$ as an example, the proposed intercept metric from (25) is illustrated for the 4 communication waveforms over the $NM = 200$ dimensional space. Finally, varying degrees of relative sampling offset is considered to discern the robustness of the set of waveforms generated by each technique.

A. Symbol Error Rate

As an example, we consider signal-to-interference ratio (SIR) values of -30 dB, -35 dB, and -40 dB and vary the signal-to-noise ratio (SNR) from -15 dB to 0 dB. The symbol error rate (SER) results for the three different waveform design techniques used in conjunction with the matched filter and decorrelator receivers, respectively, are presented in Figs. 5, 6, and 7. Note that the same sets of weight vectors \mathbf{b}_k and pseudo-random vectors \mathbf{d}_k for the WC and DP approaches, respectively, are used throughout the evaluation of symbol error rate.

It is observed in Fig. 5 for the eigenvectors-as-waveforms (EAW) approach that the per-

formance for the matched filter and decorrelator receivers is identical. This result is expected because, with an $M = 2$ over-sampling factor, the $K = 4$ eigenvectors with the smallest associated eigenvalues have very little correlation with the ambient radar scattering. Thus the interference cancellation capability of the decorrelator is not necessary in this case. However, as will be shown in Section VI.B, the near-orthogonality between the communication waveforms and the ambient scattering can be quite detrimental to the intercept probability.

In comparison to the EAW approach, the weighted-combining (WC) and dominant-projection (DP) waveform design techniques in Figs. 6 and 7, respectively, yield higher symbol error rates, with DP performing marginally better than WC. This result is also expected because the WC and DP approaches use a considerably larger portion of the waveform design space (we set $L = 100$ in this case) and thus are somewhat more correlated with the ambient scattering. Due to this higher correlation, the SER performance of the matched filter is found to be rather poor (the symbol error rate remains above 10^{-2} for all three SIR values considered). However, the interference cancellation capability of the decorrelator is demonstrated with the achievement of a 10^{-3} symbol error rate for $\text{SIR} = -30$ dB and $\text{SNR} = -8$ dB with both waveform design approaches. It is this ability to employ interference cancellation at the intended receiver and thereby achieve a sufficiently low symbol error rate for these interference-masked signals that signifies the utility of intra-pulse radar-embedded communications.

B. Intercept Metric

To characterize the intercept properties of the three proposed waveform design techniques, we shall use the intercept metric described in Section V.B. The EAW waveforms are the same as those used in Section VI.A. Due to the different possibilities for the weight vectors \mathbf{b}_k and pseudo-random vectors \mathbf{d}_k for the WC and DP approaches, respectively, 10 different sets of each used so as to reduce the variation of set selection with respect to the intercept metric. For each set of $K = 4$ waveforms, 100 independent trials are performed with different interference and noise distributions (drawn from a complex Gaussian distribution as before). The signal-to-interference ratio (SIR) is set to -35 dB and the signal-to-noise ratio (SNR) is set to -10 dB. Without loss of generality, the $k = 1$ communication waveform is added to the noise and interference to yield the received signal as in (17) that is used to ascertain the intercept metric via (24) and (25).

Figures 8, 9, and 10 illustrate the results of this intercept metric for the EAW, WC, and DP waveforms, respectively. It is observed that the normalized correlation value for the EAW

waveform actually reaches unity when all but the rank-4 space occupied by the communication waveforms has been projected out of the received signal. Thus an intercept receiver could conceivably obtain an exact replica of the embedded communication waveforms. We may thereby infer that the EAW approach does not provide waveforms that have a low probability of intercept.

It was shown in Section VI.A that the WC and DP waveforms result in some symbol error rate degradation relative to the EAW waveforms. The result of this trade-off in receive error performance is the significantly lower correlation values for the WC and DP waveforms as evidenced in Figs. 9 and 10. The peak normalized correlation values for WC and DP are 0.235 and 0.244, respectively. As such, we may infer that an intercept receiver, presumed to possess no prior knowledge of the set of embedded communication waveforms, would have virtually no ability to determine either the presence of these waveforms or their properties. Also, note that compared to the correlation values evoked by waveform $k = 1$, the correlation values for waveforms $k = 2, 3$, and 4 are even smaller with a maximum value of 0.095 for both WC and DP. Hence, by employing coherent processing (by virtue of possessing prior knowledge of the set of communication waveforms) the intended receiver may readily discern which of the given waveforms is truly present in the received signal.

C. Sampling Offset Robustness

Finally, we consider an implementation issue that could potentially be quite detrimental to performance at the intended receiver. As discussed in Section V, there exists the possibility that the illuminating radar waveform received at both the tag and at the intended receiver may be sampled such that there may be a relative offset between the respective discrete representations of \mathbf{s} . If this sampling offset occurs then there will be differences between the sets of eigenvectors determined at each location.

To ascertain the degradation of a sampling offset we shall generate delayed versions of the continuous radar waveform $s(t)$ and subsequently sample these versions at the same rate to obtain length- NM “offset” radar waveforms. The amount of delay is set relative to the Nyquist complex sampling interval of $T = \frac{1}{B}$. Thus, we consider delays of $\Delta T = 0$ (*i.e.* no offset), $\Delta T = \frac{0.5}{B}$, and $\Delta T = \frac{1}{B} = T$. Given the ability of the tag and intended receiver to synchronize with the pulse repetition interval (PRF) of the illuminating radar, it is expected that greater relative offset is unlikely. Also, by invoking symmetry only positive values of delay need be considered.

For the purpose of simulation, we shall assume that the tag possesses the radar waveform representation used in Section VI.A and the intended receiver possesses an offset-sampled version of the radar waveform. The P3 radar waveform provides a mathematical function that can easily be manipulated to produce “offset-sampled” versions of the discrete radar waveform representation (note that if $\Delta T \geq \frac{1}{MB}$ then zeroes must be inserted into the offset discrete representation to account for the finite pulse-width of the radar waveform). For the offset-sampled radar waveform \mathbf{s}_{off} produced by each of the delays above, the corresponding matrix \mathbf{S}_{off} is constructed as (8) from which a correlation matrix is formed and the eigen-decomposition subsequently computed as in (9). The set of resulting eigenvectors, denoted as \mathbf{V}_{off} , are used to generate the communication waveforms $\mathbf{c}_{k,\text{off}}$ for each of the three techniques to be used at the receiver. The signal-to-interference ratio (SIR) is set at -35 dB and the signal-to-noise ratio (SNR) is varied between -15 dB and 0 dB to determine symbol error rate performance for each of the three waveform design techniques for different degrees of sampling offset.

Figures 11, 12, and 13 depict the receiver error performance for the eigenvalues-as-waveforms (EAW), weighted-combining (WC), and dominant-projection (DP) approaches, respectively. The EAW approach is found to experience the most severe degradation when sampling offset occurs. For example, at an SNR of -5 dB, the symbol error rate increases by more than an order of magnitude for a sampling offset of $\Delta T = \frac{0.5}{B}$ relative to when no offset is present. For a sampling offset of $\Delta T = \frac{1}{B}$, the symbol error rate degrades by 3 orders of magnitude relative to no offset. Because it accounts for more of the non-dominant space, the degradation for the WC approach is less severe. At -5 dB SNR, a sampling offset of $\Delta T = \frac{0.5}{B}$ nearly doubles the symbol error rate for WC while a sampling offset of $\Delta T = \frac{1}{B}$ increase the symbol error rate by an order of magnitude.

The DP approach suffers the least degradation because it does not address the individual eigenvectors instead utilizing a sub-space as a whole. At -5 dB SNR, the symbol error rate for DP nearly doubles for a sampling offset of $\Delta T = \frac{1}{B}$. When the sampling offset is $\Delta T = \frac{0.5}{B}$, the symbol error rate increase is negligible. Thus, of the three proposed waveform design techniques, the dominant-projection approach has been found to be the most robust to sampling offset.

VII. CONCLUSIONS

A new framework for radar-embedded communications has been presented which operates by re-modulating the signal reflected by an tag/transponder on an *intra*-pulse basis such that a

different communication symbol is embedded with each incident radar pulse. In so doing, data rates on the order of kbps may be achieved. The set of communication symbols are temporal waveforms that are designed to provide a low error rate at the intended receiver while also providing a low probability of intercept by an adversary. Three approaches for the design of these communication waveforms are described which provide varying degrees of symbol error rate performance, intercept probability, and robustness to practical implementation. Additionally, it is demonstrated that for communication waveform providing low intercept probability because they are well-masked by the ambient radar scattering, interference cancellation yields substantial symbol error rate performance gains relative to the matched filter receiver.

REFERENCES

- [1] D.L. Nicholson, *Spread Spectrum Signal Design: Low Probability of Exploitation and Anti-Jam Systems*, W.H. Freeman and Co: New York, NY, 1988.
- [2] H. Stockman, "Communication by means of reflected power," *Proceedings of the IRE*, vol. 36, no. 10, pp. 1196-1204, Oct. 1948.
- [3] D.M. Dobkin, *The RF in RFID*, Elsevier, Inc., New York, NY, 2008, pp. 34-35.
- [4] M. Soumekh, "SAR-ECCM using phase-perturbed LFM Chirp signals and DRFM repeat jammer penalization," *IEEE Trans. on Aerospace and Electronic Systems*, 42(1), pp. 191-205, 2006.
- [5] D.R. Brunfeldt and F.T. Ulaby, "Active reflector for radar calibration," *IEEE Trans. on Geoscience and Remote Sensing*, 22(2), pp. 16-169, 1984.
- [6] A. Freeman, Y. Shen, and C.L. Werner, "Polarimetric SAR calibration experiment using active radar calibrators," *IEEE Trans. on Geoscience and Remote Sensing*, 28(2), pp. 224-240, 1990.
- [7] M. Fujita, "Development of a retrodirective PARC for ALOS/PALSAR calibration," *IEEE Trans. Geoscience and Remote Sensing*, vol. 41, no. 10, pp. 2177-2186, Oct. 2003.
- [8] M. Fujita and S. Nakamura, "A polarization-rotating Van Atta array reflector and its application to polarimetric radar calibration," in proc. *IEEE Intl. Geoscience and Remote Sensing Symp.* pp. 1746-1749, 2004.
- [9] R.M. Axline, G.R. Sloan, and R.E. Spalding, "Radar transponder apparatus and signal processing technique," US Patent 5,486,830, 23 Jan 1996.
- [10] D. Hounam and K.H. Wagel, "A technique for the identification and localization of SAR targets using encoding transponders," *IEEE Trans. Geoscience and Remote Sensing*, vol. 39, no. 1, pp. 3-7, Jan. 2001.
- [11] D.L. Richardson, S.A. Stratmoen, G.A. Bendor, H.E. Lee, and M.J. Decker, "Tag communication protocol and system," US Patent 6,329,944, 11 Dec 2001.
- [12] R.M. Axline, G.R. Sloan, and R.E. Spalding, "Transponder data processing methods and systems," US Patent 6,577,266, 10 Jun 2003.
- [13] R.C. Ormesher and R.M. Axline, "Methods and system suppressing clutter in a gain-block, radar-responsive tag system" US Patent 7,030,805, 18 Apr 2006.

- [14] R. Bracht, E.K. Miller, and T. Kuckertz "An impedance-modulated reflector system," *IEEE Potentials*, 18(4), pp. 29-33, 1999.
- [15] K.M.K.H. Leong, Y. Wang, and T. Itoh, "A full duplex capable retrodirective array system for high-speed beam tracking and pointing applications," *IEEE Trans. Microwave Theory and Techniques*, vol. 52, no. 5, pp. 1479-1489, May 2004.
- [16] S.D. Blunt and P. Yatham, "Waveform design for radar-embedded communications," *proc. of Intl. Waveform Diversity and Design Conf.*, pp. 214-218, June 4-8, 2007.
- [17] S.D. Blunt, J. Stiles, C. Allen, D. Deavours, and E. Perrins, "Diversity aspects of radar-embedded communications," *proc. of Intl. Conf. on Electromagnetics in Advanced Applications*, Sept. 17-21, 2007.
- [18] L.M. Supplee, R.P. Cohn, J.S. Collura, and A.V. Macree, "MELP: The new federal standard at 2400 bps," in *proc. Intl. Conf. on Acoustics, Speech, and Signal Processing*, pp. 1591-1594, Apr. 1997.
- [19] T. Wang, K. Koishida, V. Cuperman, A. Gersho, and J.S. Collura, "A 1200 bps speech coder based on MELP," in *proc. Intl. Conf. on Acoustics, Speech, and Signal Processing*, pp. 1375-1378, June 2000.
- [20] M.W. Chamberlain, "A 600 bps MELP vocoder for use on HF channels," in *proc. Military Communications Conf.*, pp. 447-453, Oct. 2001.
- [21] S. Verdú, *Multiuser Detection*, Cambridge University Press, Cambridge, UK, 1998.
- [22] R. Lupas and S. Verdú, "Linear multiuser detectors for synchronous code-division multiple-access channels," *IEEE Trans. Information Theory*, vol. 35, pp. 123-136, Jan. 1989.
- [23] S.M. Kay *Fundamentals of Statistical Signal Processing: Estimation Theory*, Chapter 7, Prentice Hall, Upper Saddle River, NJ, 1993.
- [24] S.M. Kay *Fundamentals of Statistical Signal Processing: Detection Theory*, Chapter 4, Prentice Hall, Upper Saddle River, NJ, 1993.
- [25] J. de Graaf, H. Faust, J. Alatishe, and S. Talapatra, "Generation of spectrally confined transmitted radar waveforms: experimental results," in *proc. IEEE Radar Conf.*, Apr. 2006.
- [26] P.E. Pace, *Detecting and Classifying Low Probability of Intercept Radar*, Artech House, Norwood, MA, 2004, pp. 135-145.

FIGURES

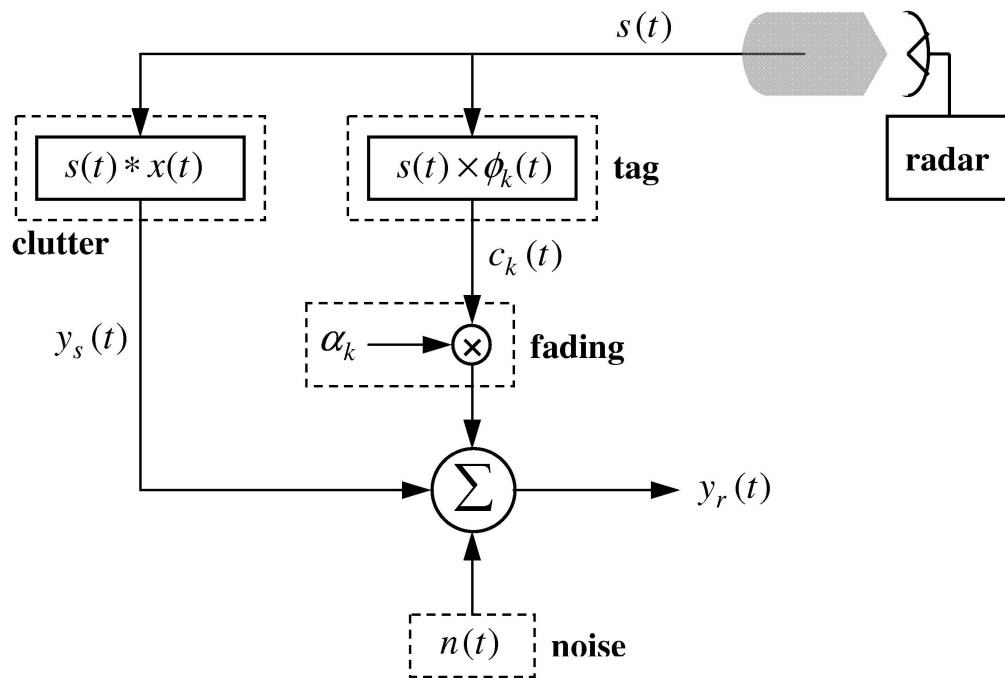


Fig. 1. Notional operation of an intra-pulse re-modulating tag and relevant phenomenology

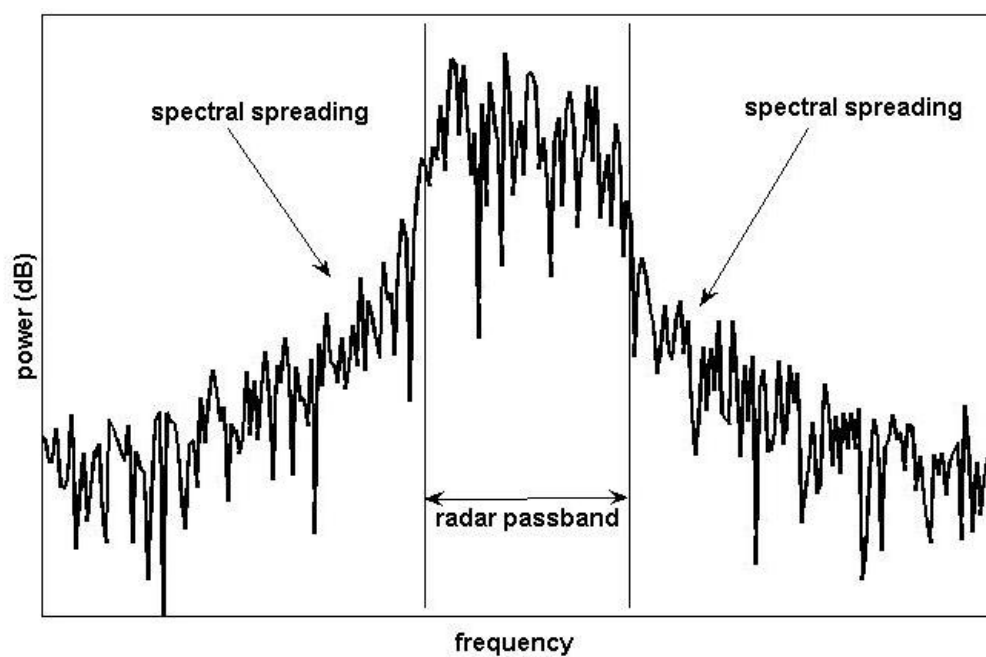


Fig. 2. Radar spectral "spreading" effect

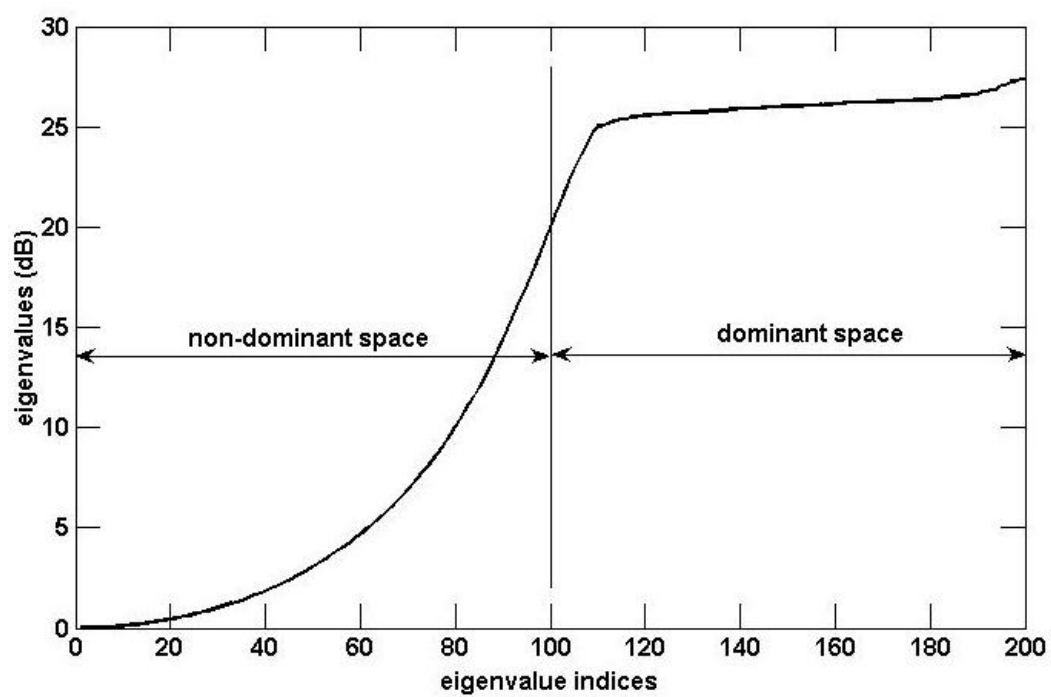
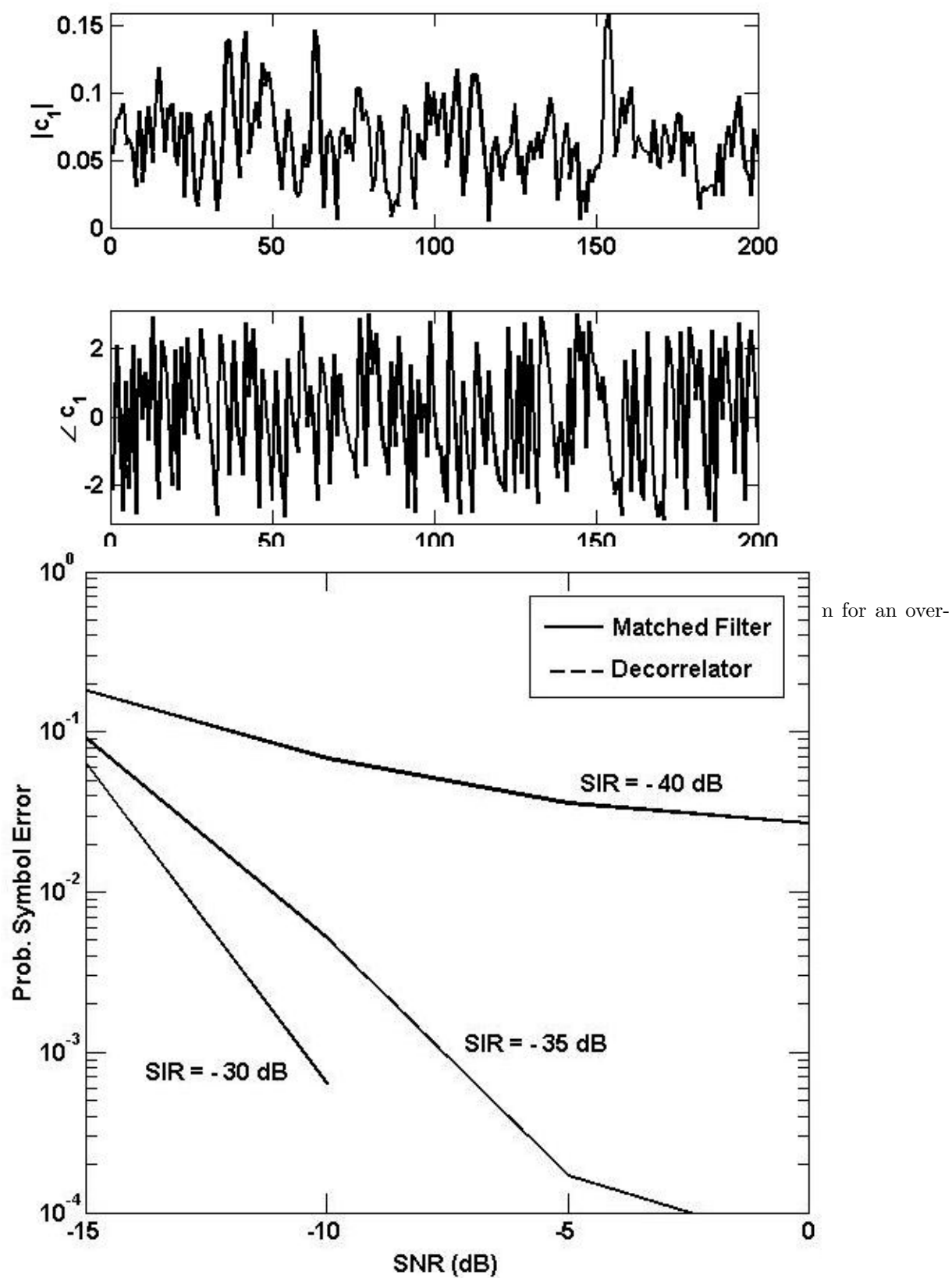


Fig. 3. Eigenvalues of correlation matrix for $M = 2$ over-sampled LFM



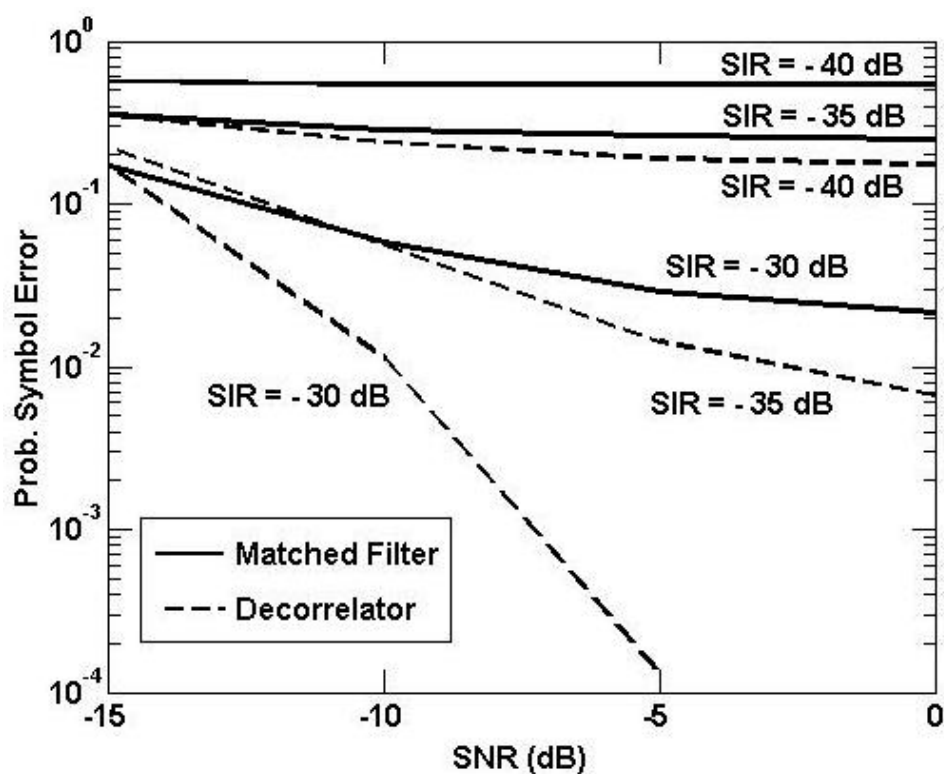


Fig. 6. Symbol-error-rate for weighted-combining waveform design

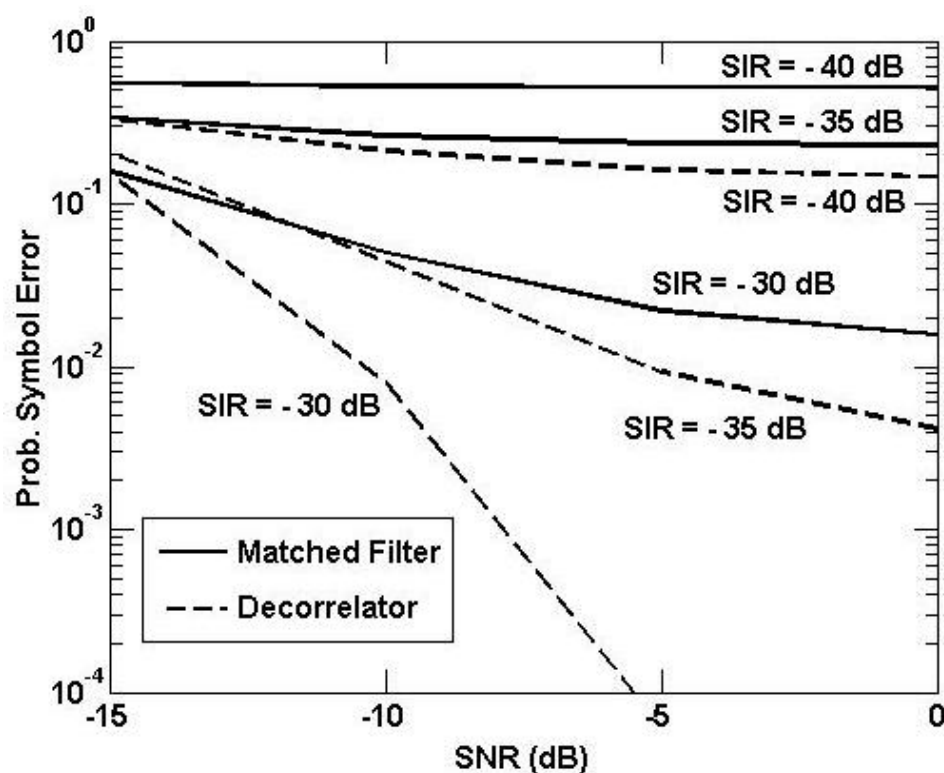


Fig. 7. Symbol-error-rate for dominant-projection waveform design

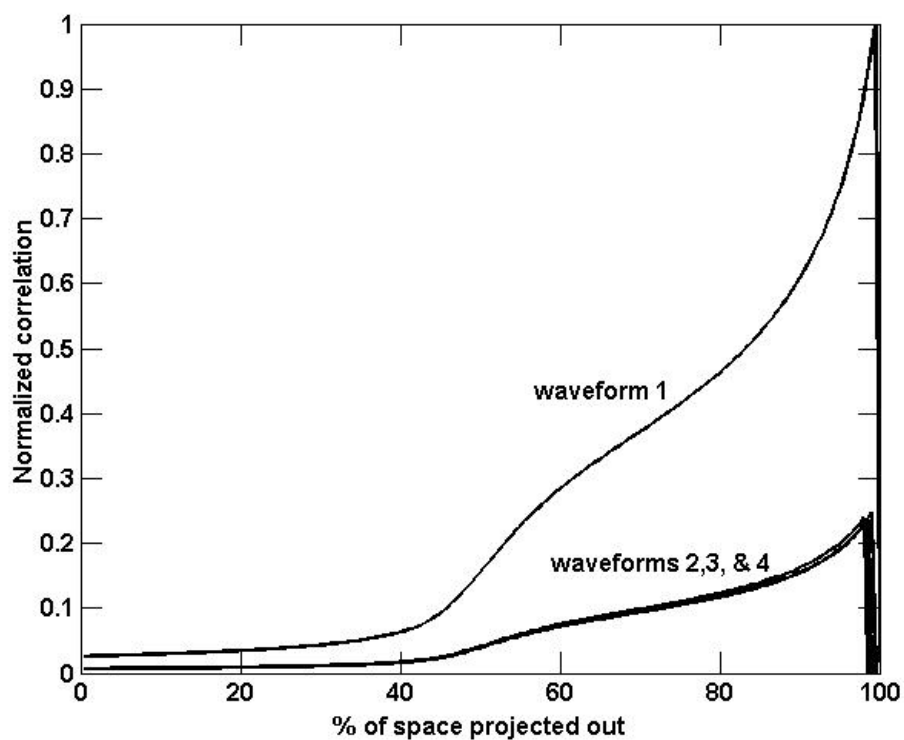


Fig. 8. Intercept metric for eigenvalues-as-waveforms waveform design

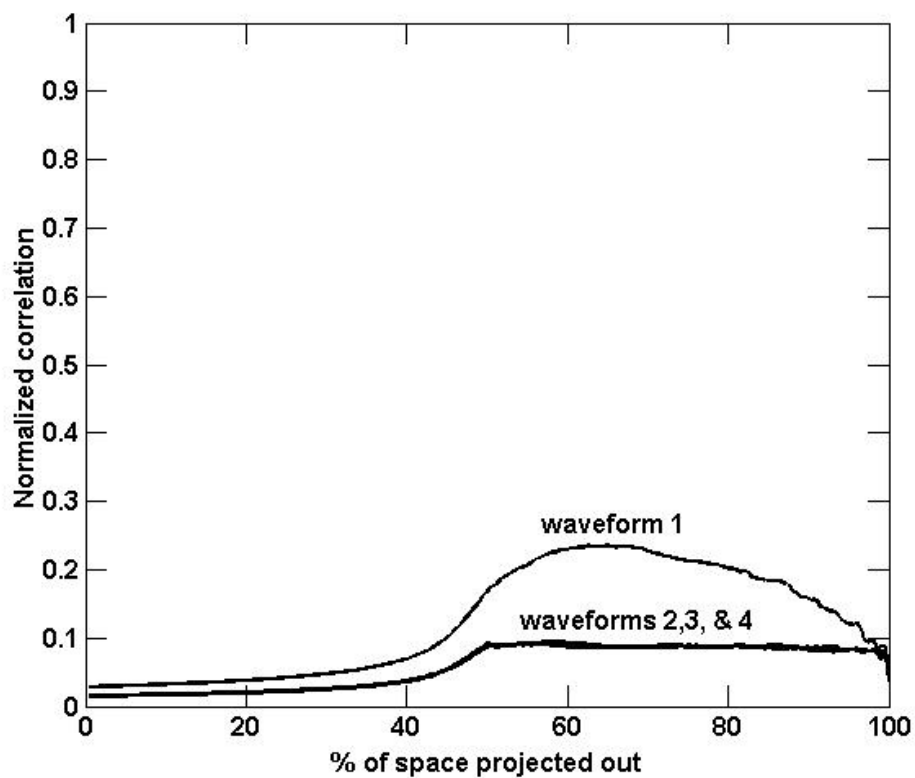


Fig. 9. Intercept metric for weighted-combining waveform design

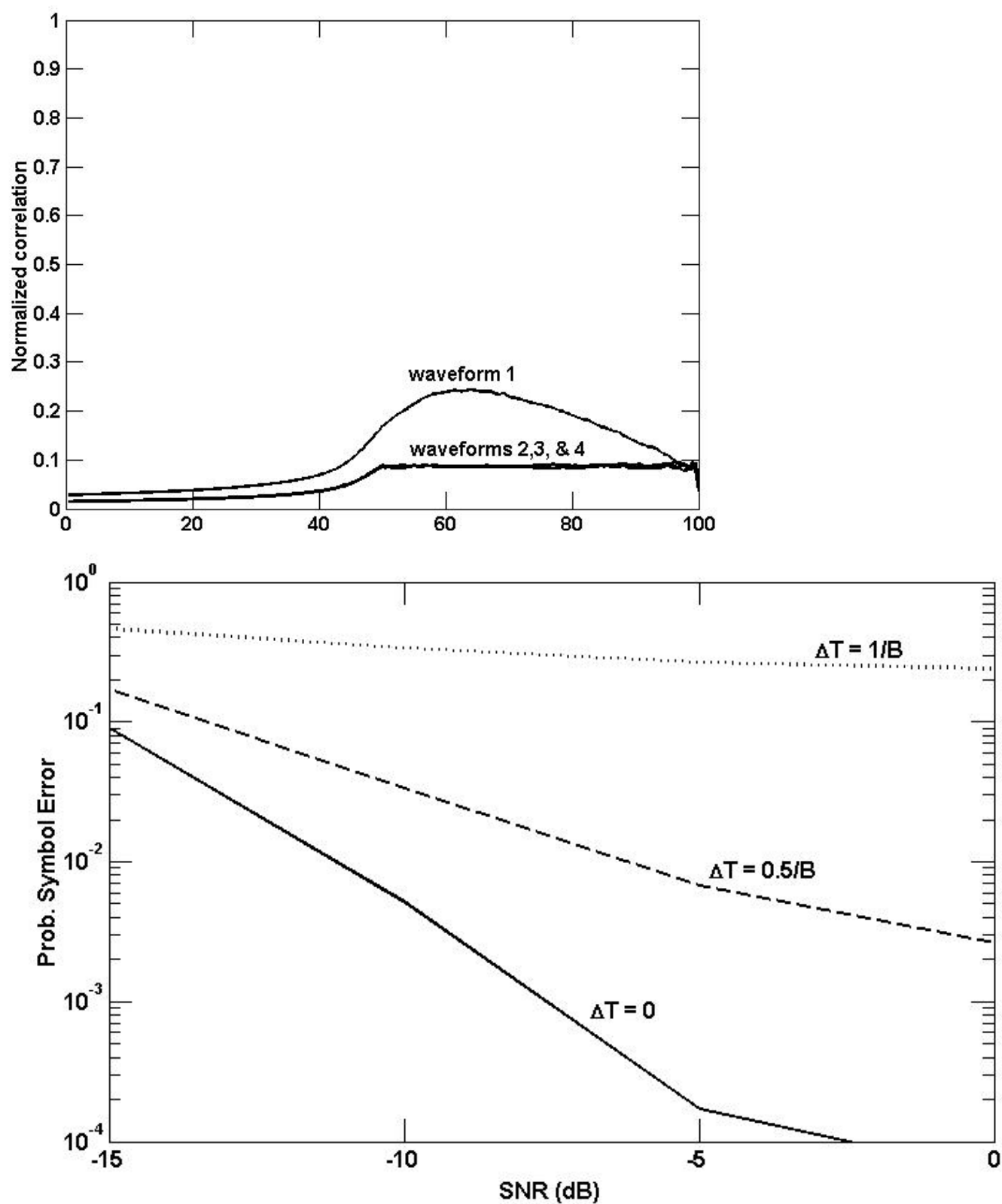


Fig. 11. Symbol-error-rate robustness to sampling-offset for eigenvalues-as-waveforms waveform design

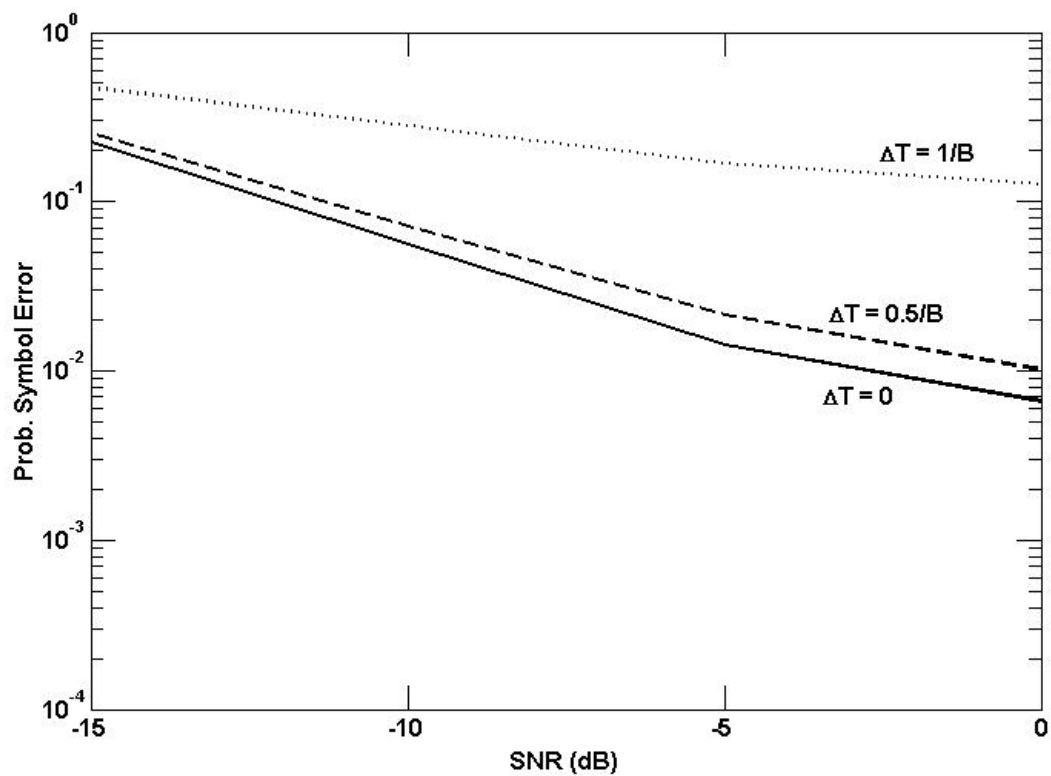


Fig. 12. Symbol-error-rate robustness to sampling-offset for weighted-combining waveform design

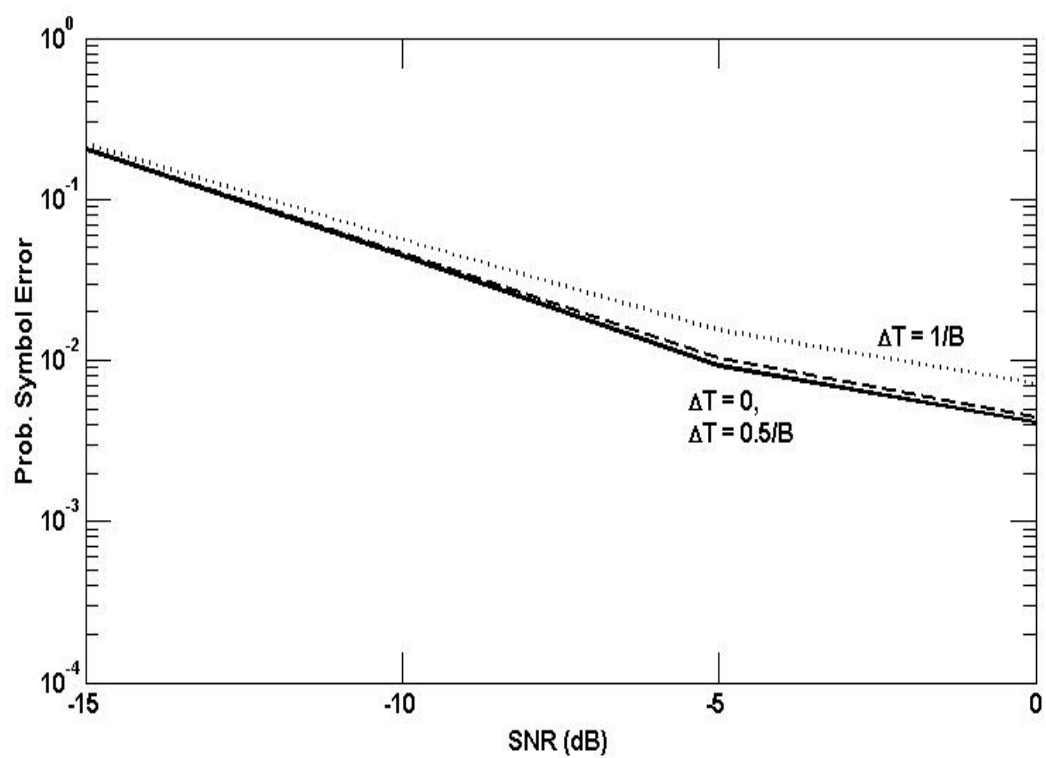


Fig. 13. Symbol-error-rate robustness to sampling-offset for dominant-projection waveform design